**PREDICTED BURIED WATER ICE STABILITY REGIONS FOR THE MOON'S POLES FROM THE DIVINER LUNAR RADIOMETER.** M.E. Landis[1*], P.O. Hayne[1], J.-P. Williams[2], B.T. Greenhagen[3], D.A. Paige[2]. [1]Laboratory for Atmospheric and Space Physics, University of Colorado, Boulder, CO, USA (*margaret.landis@lasp.colorado.edu), [2]Department of Earth, Planetary and Space Sciences, University of California, Los Angeles, CA, USA, [3]Johns Hopkins University Applied Physics Laboratory, Laurel, MD, USA.

**Introduction:** The origin of lunar polar volatiles is a long-standing mystery in planetary science, especially as these volatiles may hold a key to understanding volatile delivery, composition, and timing to Earth and/or be a laboratory for understanding the effect of volcanism on rocky planet interior degassing. Direct measurements and inferences from remote sensing have indicated that water ice and other volatiles exist in the near-subsurface of the lunar south polar region (e.g., [1-6]). Neutron data suggest hydrogen enhancement at both poles (e.g., [7]), consistent with the presence of buried water ice or hydrated minerals in the upper ~1 m of the surface. Buried water ice may explain trends in lunar crater depth-to-diameter ratios with latitude [8] and could record previous lunar polar orientations [9]. One outstanding issue is how now-buried hydrogen could have been delivered to the subsurface and when.

This work addresses one aspect of the buried lunar hydrogen problem: Are predictions of the thermal stability of buried water ice within the ~1 m of the surface from Diviner radiometer data consistent with the hydrogen distribution observed in the present day? If not, where do they differ and by how much? We present results from processing the Diviner data and using a minimal thermal model to refine predictions of subsurface temperature and buried water ice stability for comparison with other orbital data sets.

**Data:** We use two Diviner-derived data sets: maximum temperature [10] and annual average temperature over the course of 10 Draconic years. We use the latitude range of 60-90° to be able to ultimately apply the smaller Diviner footprint (~300 m) to the larger regional-scale footprints from neutron instruments like the one on Lunar Prospector [e.g., 11].

We calculate annual average temperature by averaging the data in bins of ~1 terrestrial day (360 bins/year) in order to reduce the effect of noise in the radiance measurements on the final bolometric temperature calculations and to minimize variations in local time in each binned average. To determine temperature, we follow the techniques described in [1]. We average each of the 360 resulting bolometric temperature maps together to generate the yearly maps. This reduces the number of local time bins used in previous work [12] and does not correct for bias in local time sampling, though the final annual average bolometric temperatures and temperature distributions at the south pole are in good agreement. The average temperature map for both poles are shown in Figure 1.

***Figure 1.*** *Annual average bolometric temperature for the lunar poles from 60-90° latitude using 360 bins per year, derived from Diviner radiance data. Concentric circles mark every 5° of latitude.*

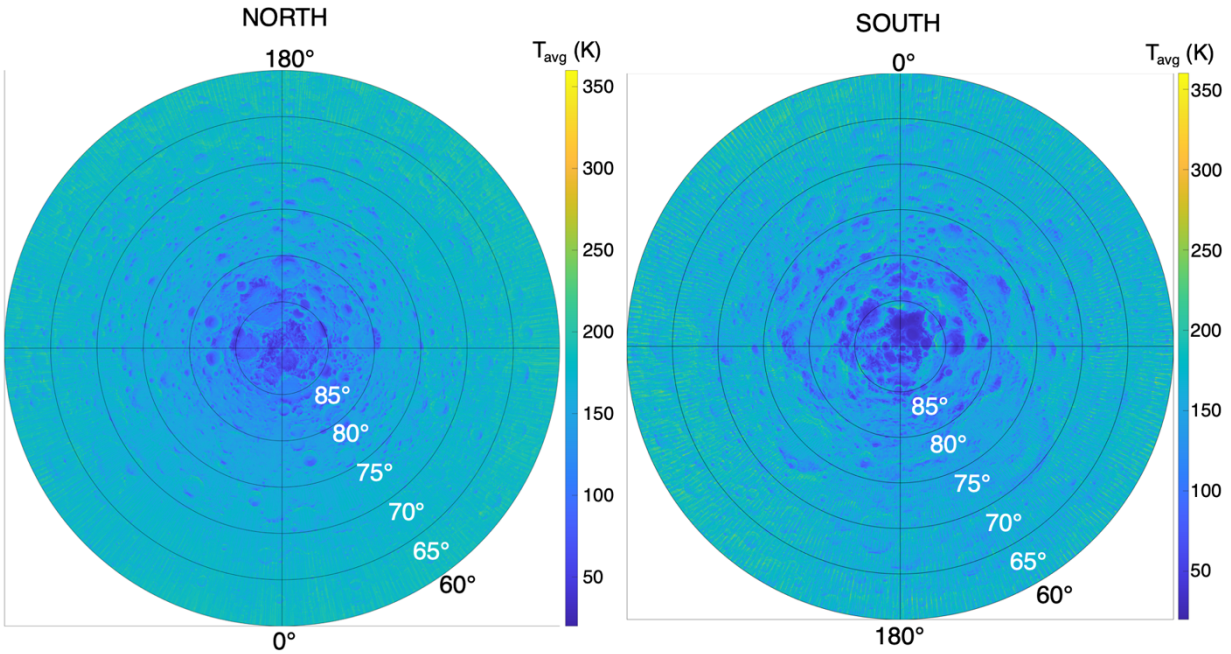

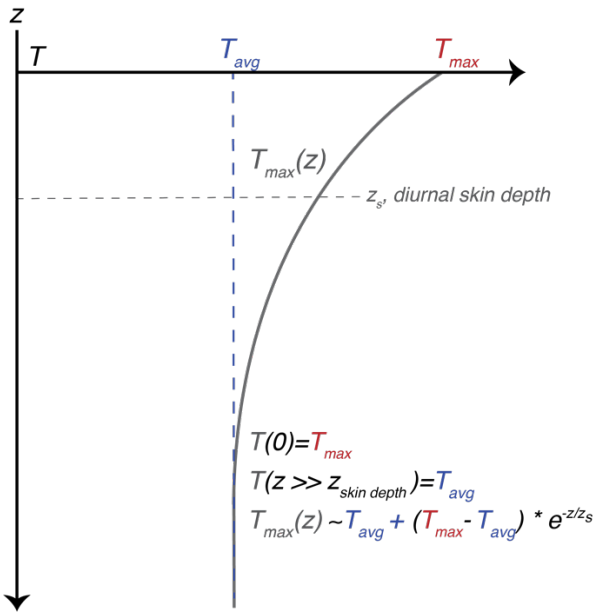


***Figure 2.*** *Schematic showing our assumptions behind calculating lunar subsurface temperature. This temperature calculation is used to determine the predicted vapor flux of a water ice deposit at this location, and therefore its long-term stability.*

**Minimal thermal and vapor loss model:** We model the temperature decay in the subsurface using a simple model (Figure 2) rather than a full 3D thermal model or assuming that the annual average temperature is representative of typical temperatures in very near-surface regions (< 1 m). This provides a data-reliant method for calculating temperatures (and therefore water vapor loss) especially for regions where water ice may be stable near or within the diurnal skin depth (e.g., ~4-7 cm, though in some places closer to ~10 cm [13]).

We assumed that the subsurface annual temperature curve could be calculated by setting the top of the surface to the maximum temperature and that at some depth (z), the temperature would equilibrate to the annual average surface temperature. We assumed an energy balance for the overall temperature at depth that included the exponential decay of the surface temperature, the annual average temperature, and geothermal heat flux. A schematic of our assumed temperature decay with depth is shown in Figure 2.

To calculate where water ice would be stable in the subsurface, we utilize a cutoff of < 1 mm/Gyr equivalent water vapor loss. We use a Knudsen vapor diffusion scheme from [14]. In order to determine at what depth the vapor loss rate is ≤ 1 mm/Gyr, we use a Newton root finding method on each pixel in the map (0.01° grid for the 30° polar projections shown in Figure 1). Results for the south pole are shown in Figure 3. In the 80-90° S latitude range, there is generally good agreement with previous work [1] though there are locations on poleward facing slopes where our model predicts more < 1 m depth stability regions.

As we do not use time-extrapolation to compensate for Diviner's uneven sampling of local times due to orbital constraints from Lunar Reconnaissance Orbiter, small variations in temperature may be occurring that affect the $T_{max}$ and $T_{avg}$ values used in the model. At the conference, we will present sensitivity tests to small (≤ ~5 K) variations in $T_{avg}$ and $T_{max}$, as well as buried water ice results from the north pole.

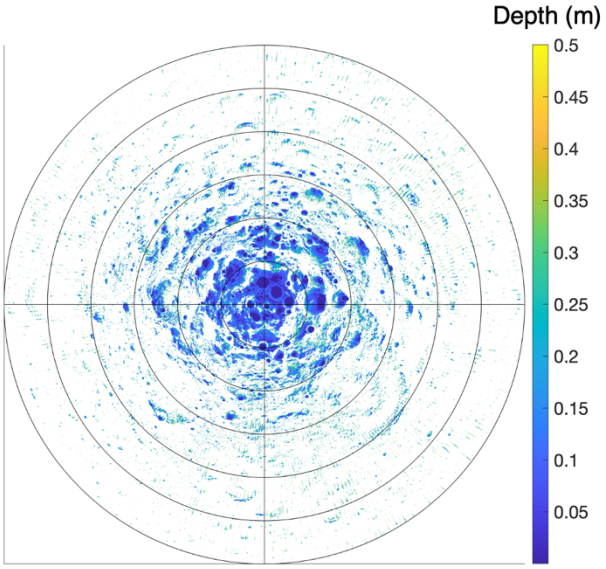


***Figure 3.*** *Depth-to-water-ice stability regions (<1 mm/Gyr vapor loss) for the lunar south pole based on a minimal thermal model and Diviner maximum and annual average temperatures.*

**Acknowledgments:** This work was supported by the Lunar Reconnaissance Orbiter Diviner project.

**References:** [1] Paige, D.A., et al. (2010). Science, 330(6003) [2] Colaprete, A., et al. (2005). Nature, 435 [3] Hayne, P.O., et al. (2010). Science, 330(6003) [4] Pieters, C.M., et al. (2009). Science, 326(5952) [5] Schultz, P.H., et al. (2010). Science, 330(6003) [6] Sefton-Nash, E., et al. (2019). Icarus, 332 [7] Feldman, W.C., et al. (1998). Science, 281(5382) [8] Rubanenko, L., et al. (2019). Nature Geoscience, 12(8) [9] Siegler, M.A., et al. (2016). Nature, 531(7595) [10] Landis, M.E., et al. (2022). The Planetary Science Journal, 3(2) [11] Feldman, W.C., et al. (2000). JGR:Planets, 105(E2) [12] Williams, J.P., et al. (2019). JGR: Planets, 124(10) [13] Hayne, P.O., et al. (2017). JGR: Planets, 122(12) [14] Schorghofer, N. (2008). The Astrophysical Journal, 682(1)